Electronic Supplementary Information

Influence of structure-selective fluorene-based polymer wrapping on optical transitions of single-wall carbon nanotubes

Masayoshi Tange,[*a] *Toshiya Okazaki*[*a] *and Sumio Iijima*[a]

[a] Nanotube Research Center, National Institute of Advanced Industrial Science and Technology (AIST),

Tsukuba 305-8565, Japan

E-mail: masa-tange@aist.go.jp; toshi.okazaki@aist.go.jp

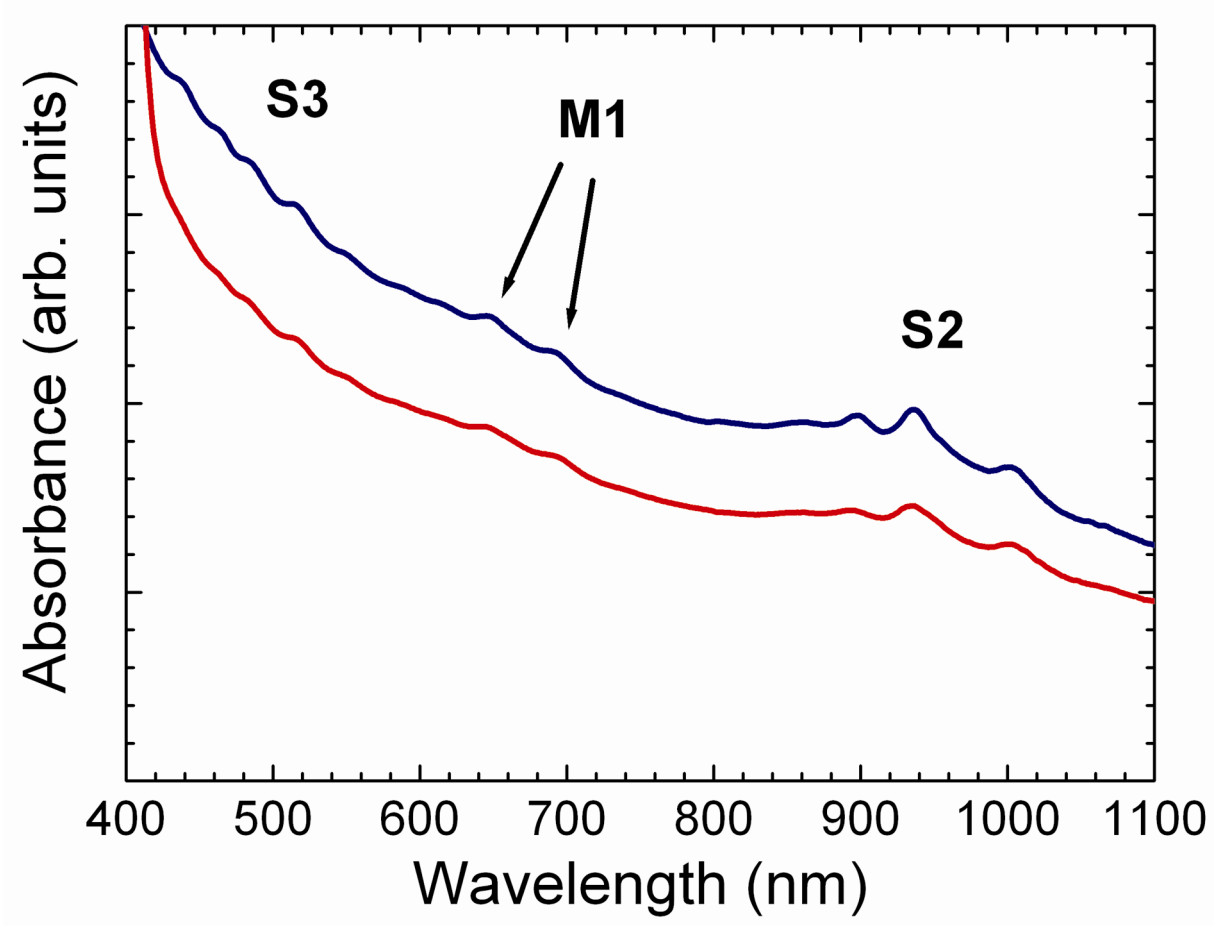

Fig. S1 Absorption spectra of PLV-SWCNTs dispersed in toluene by PFOPy (blue line) and PFD (red line) before ultracentrifugation. The absorption bands indicated by S3, S2, and M1 are respectively attributed to the third and second optical transitions of semiconducting tubes and the first optical transitions of metallic tubes.

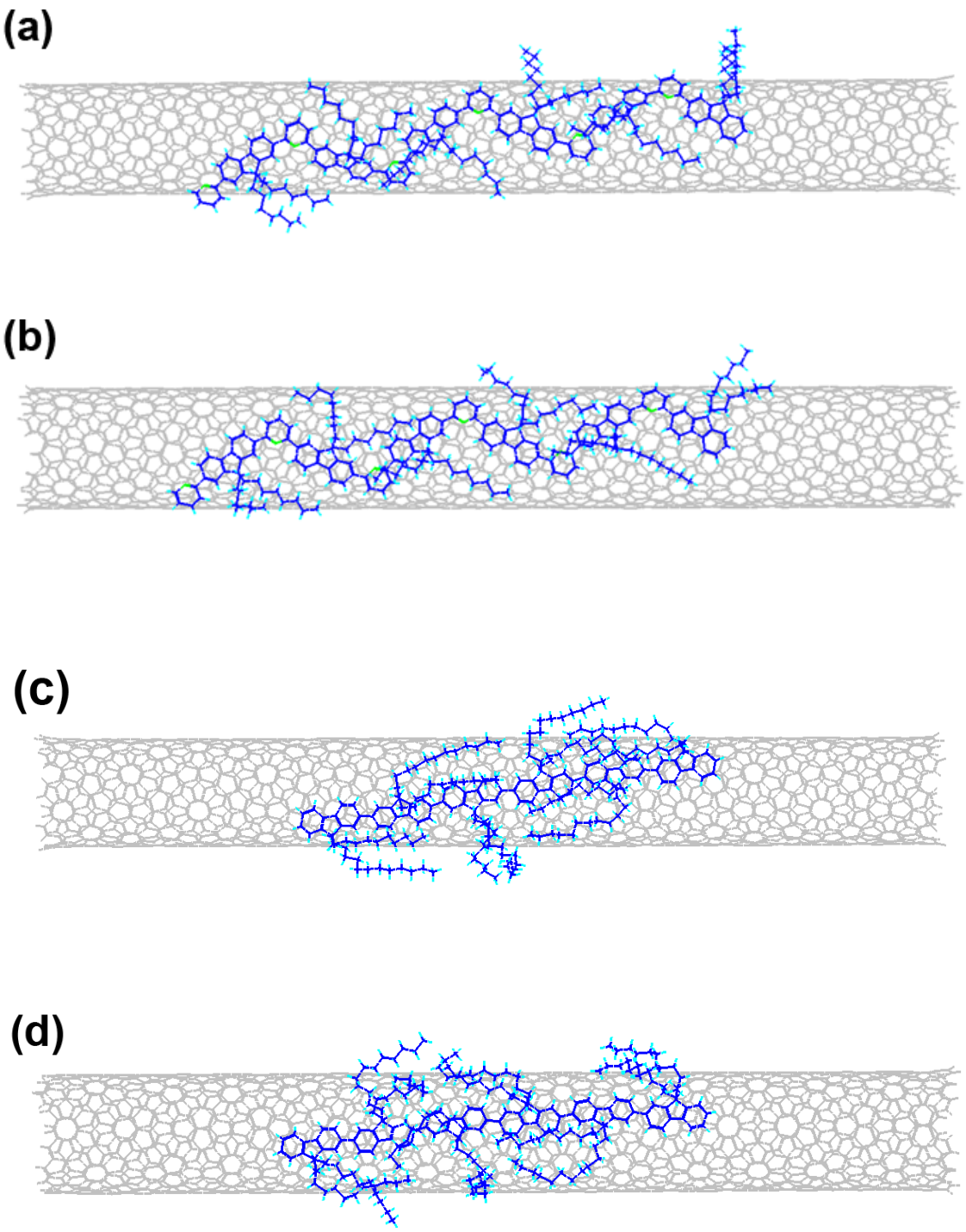

Fig. S2 Simulated configurations of individual oligomers and large-diameter SWCNT: (a) a fluorene-pyridine sixmer and a (13,5) SWCNT,[1] (b) a fluorene-pyridine sixmer and a (15,4) SWCNT, (c) a fluorene sixmer and a (13,5) SWCNT, and (d) a fluorene sixmer and a (15,4) SWCNT.

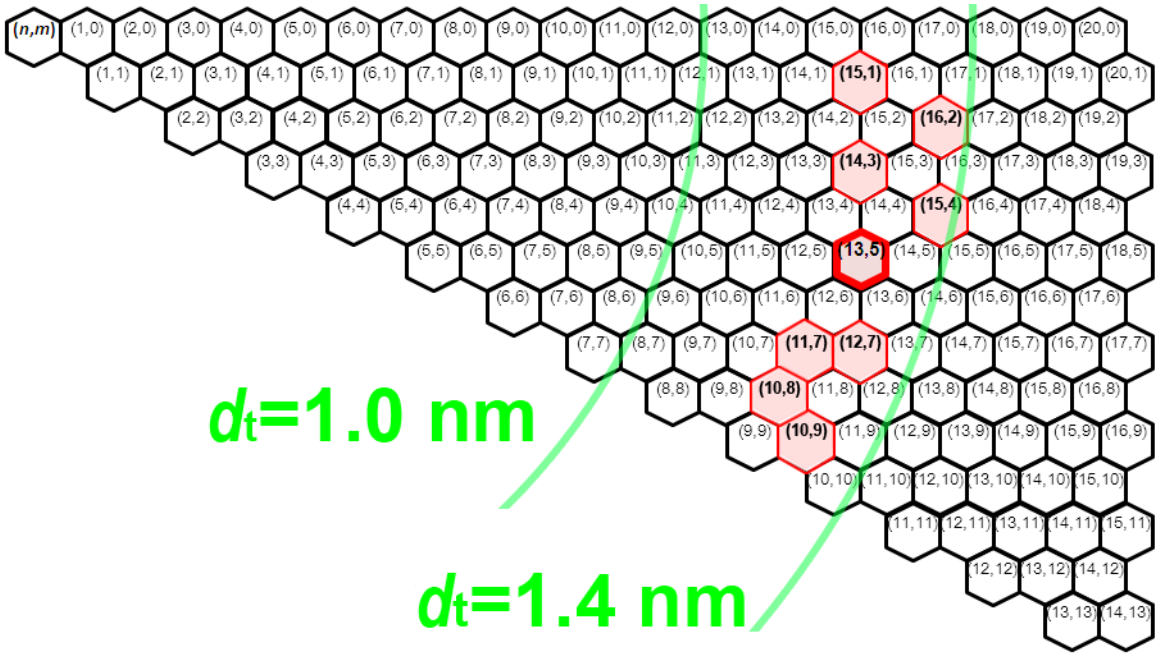

Fig. S3 Graphene sheet map showing the (*n*,*m*) species of PFOPy-extracted SWCNTs in toluene. The species of the extracted SWCNTs are denoted by red hexagons. The most prominent species in the PLE map is indicated by a thick hexagon.

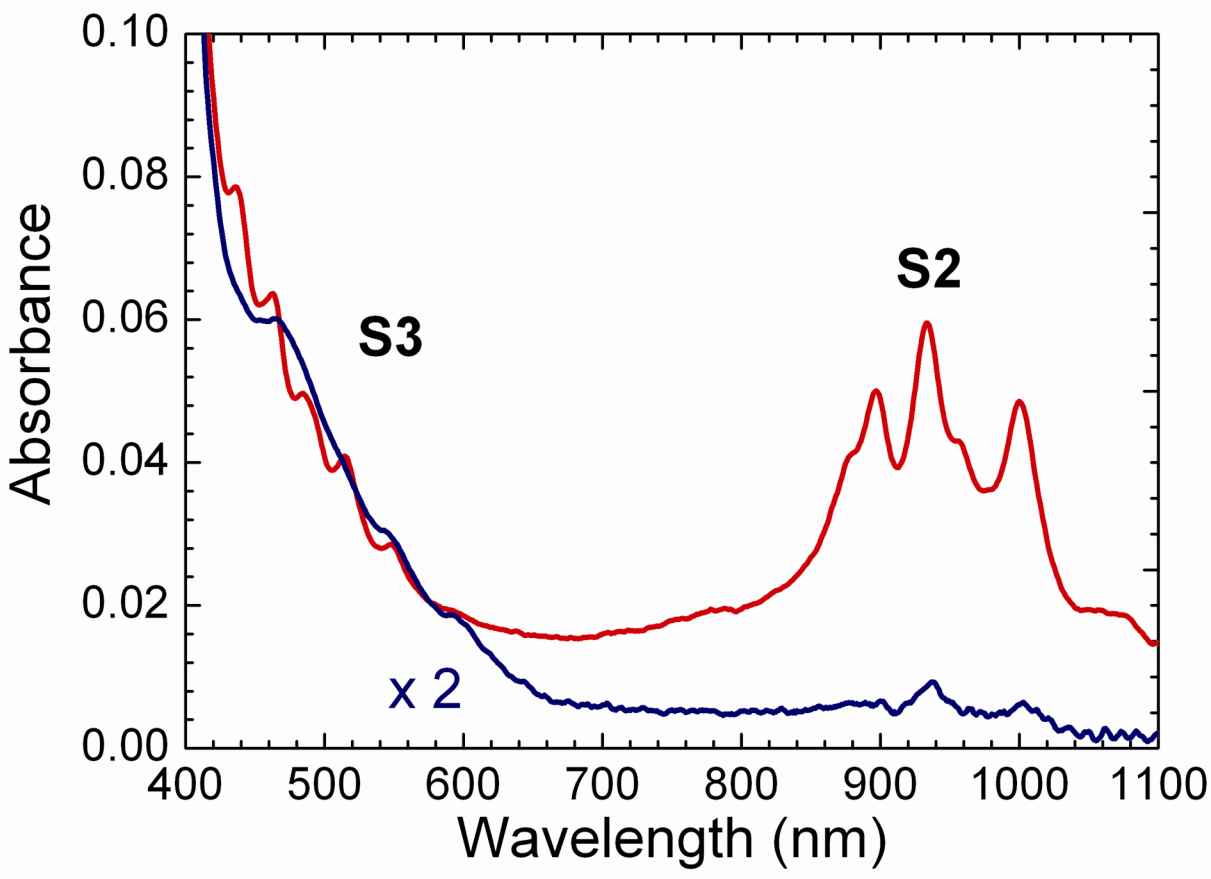

Fig. S4 Absorption spectra of PFOPy-extracted SWCNTs in toluene (blue line) and *p*-xylene (red line). The absorption bands indicated by S3 and S2 are attributed to the third and second optical transitions of semiconducting tubes, respectively. The absorption backgrounds in short wavelengths near 400 nm are significantly increased by the absorption of PFOPy.

Table S1. PL peak positions of PFD-wrapped PLV-SWCNTs in toluene.

(*n*,*m*)	Excitation wavelength (nm)	Emission wavelength (nm)	(*n*,*m*)	Excitation wavelength (nm)	Emission wavelength (nm)
(8,6)	726	1193	(13,2)	873	1333
(8,7)	744	1282	(13,3)	771	1509
(9,7)	802	1342	(13,5)	935	1512
(9,8)	822	1432	(13,6)	894	1654
(10,6)	768	1396	(13,8)	1014	1722
(10,8)	880	1494	(14,3)	934	1474
(10,9)	902	1577	(14,4)	864	1634
(11,6)	869	1423	(14,6)	1011	1651
(11,7)	854	1535	(15,1)	936	1455
(11,9)	957	1642	(15,2)	844	1634
(11,10)	985	1725	(15,4)	1003	1616
(12,4)	865	1363	(15,5)	940	1776
(12,5)	815	1518	(16,2)	1004	1580
(12,7)	942	1572	(16,3)	907	1758
(12,8)	937	1691			

References.

[1] M. Tange, T. Okazaki and S. Iijima, *ACS Appl. Mater. Interfaces*, 2012, **4**, 6458.